AD-A112 980 PURDUE UNIV LAFAYETTE IN SCHOOL OF MECHANICAL ENGINEERING F/G 20/4
WALL LAYER STRUCTURE AND DRAG REDUCTION: ROLE OF VISCOUS SUBLAY--ETC(U)
DEC 81 W G TIEDERMAN, D G BOGARD N00014-81-K-0210
UNCLASSIFIED PME-FM-81-2 NL

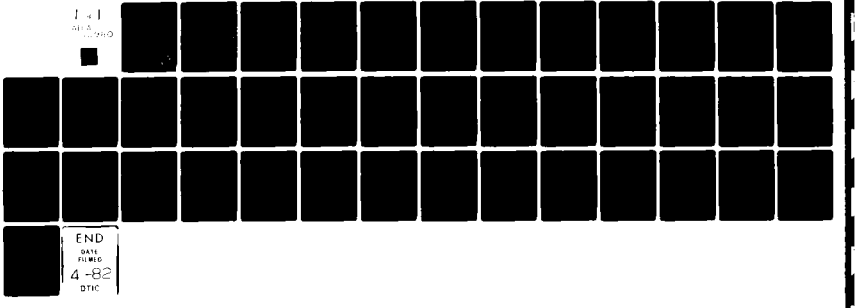

END
DATE FILMED
4-82
DTIC

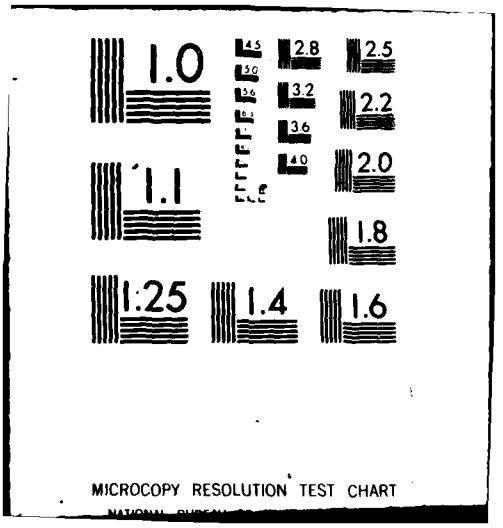
1.0
1.1
1.25
1.4
1.6
1.8
2.0
2.2
2.5
2.8
3.2
3.6
4.0
MICROCOPY RESOLUTION TEST CHART

(12)

Report PME-FM-81-2

WALL LAYER STRUCTURE AND DRAG REDUCTION

Role of viscous sublayer

William G. Tiederman and David G. Bogard
School of Mechanical Engineering
Purdue University
West Lafayette, Indiana 47907

December 1981

Technical Report for Period 02 January 1981 - 31 December 1981

Prepared for

DAVID W. TAYLOR NAVAL SHIP RESEARCH AND DEVELOPMENT CENTER
Bethesda, MD 20084

OFFICE OF NAVAL RESEARCH
800 N. Quincey St.
Arlington, VA 22217

SECURITY CLASSIFICATION OF THIS PAGE (When Data Entered)

REPORT DOCUMENTATION PAGE		READ INSTRUCTIONS BEFORE COMPLETING FORM
1. REPORT NUMBER PME-FM-81-2	2. GOVT ACCESSION NO. AD-A112 980	3. RECIPIENT'S CATALOG NUMBER
4. TITLE (and Subtitle) WALL LAYER STRUCTURE AND DRAG REDUCTION; Role of viscous sublayer		5. TYPE OF REPORT & PERIOD COVERED TECHNICAL REPORT Jan. 2, 1981 through December 31, 1981 6. PERFORMING ORG. REPORT NUMBER
7. AUTHOR(s) William G. Tiederman and David G. Bogard		8. CONTRACT OR GRANT NUMBER(s) N00014-81-K-0210
9. PERFORMING ORGANIZATION NAME AND ADDRESS School of Mechanical Engineering Purdue University West Lafayette, Indiana 47907		10. PROGRAM ELEMENT, PROJECT, TASK AREA & WORK UNIT NUMBERS SR0230101 61153N R02301
11. CONTROLLING OFFICE NAME AND ADDRESS David W. Taylor Naval Ship Research and Development Center Code 1505 Bethesda, MD 20084		12. REPORT DATE December 1981 13. NUMBER OF PAGES 36
14. MONITORING AGENCY NAME & ADDRESS(if different from Controlling Office) Office of Naval Research 800 N. Quincey St. Arlington, VA 22217		15. SECURITY CLASS. (of this report) 15a. DECLASSIFICATION/DOWNGRADING SCHEDULE

16. DISTRIBUTION STATEMENT (of this Report)
APPROVED FOR PUBLIC RELEASE: DISTRIBUTION UNLIMITED

17. DISTRIBUTION STATEMENT (of the abstract entered in Block 20, if different from Report)

18. SUPPLEMENTARY NOTES
Sponsored by the Naval Sea Systems Command General Hydromechanics Research (GHR) Program Administered by David W. Taylor Naval Ship Research and Development Center, Bethesda, MD 20084

19. KEY WORDS (Continue on reverse side if necessary and identify by block number)
Drag reduction, Turbulent wall flows

20. ABSTRACT (Continue on reverse side if necessary and identify by block number)
The basic objective of this experimental study was to deterine if the presence of a drag-reducing polymer solution in only the viscous sublayer of a turbulent channel flow of water can inhibit the formation of low-speed streaks, and thereby reduce both the production of turbulent kinetic energy and the wall shear stress. The experiments were performed in a long water channel with a 2.5 x 25 cm rectangular cross section. Drag-reducing polymer solutions, glycerin solutions (whose viscosity matched those of the polymer

DD FORM 1 JAN 73 1473 EDITION OF 1 NOV 65 IS OBSOLETE
S/N 0102-014-6601 |

SECURITY CLASSIFICATION OF THIS PAGE (When Data Entered)

solutions) and water were seeped into the viscous sublayer of the fully developed, turbulent channel flow through thin slots in both of the 25 cm walls. Flow visualization conducted immediately downstream of the slot (before the injected fluid could migrate out of the sublayer) showed that the dimensionless spanwise spacing was the same for all injected fluids. Similarly pressure drop measurements showed that drag reduction occurred only after a portion of the polymer solutions had migrated out of the viscous sublayer. Thse results indicate that the drag-reducing molecules have a direct effect on the flow structures in the buffer region of turbulent wall flows.

A

PREFACE

The authors wish to acknowledge the assistance of Robert Ellison and William Davis during the reduction of the visualization information. The SEPARAN AP-273 was provided by the Dow Chemical Company.

TABLE OF CONTENTS

INTRODUCTION

It is well-known that small concentrations of soluble long-chain polymer molecules can reduce the wall shear stress in a turbulent flow of liquid. It is also known that for dilute solutions the polymer must be somewhere near the wall for the reduction in friction to occur [1,2,3]. Despite numerous studies that have demonstrated both the feasibility and practicality of drag reduction with polymer additives, it is not yet clear exactly what feature or features of the turbulent flow are directly affected by the polymer. A significant aspect of the problem is that there is still a good deal of disagreement about the importance of various parts of the repeatable cycle of events which produce the sharp peak of turbulence production in the near-wall region. This lack of understanding of turbulent wall flows has not prevented engineers from using polymer solutions for drag reduction. However it has prevented the construction of general mathematical models, the development of reliable methods for scaling-up laboratory results and the accurate assessment of potential schemes for drag reduction such as compliant walls and grooved surfaces without a large amount of testing. The purpose of this experimental study was to gain new knowledge about the physics of drag reduction and the near-wall region of turbulent flows.

The overall objective was to clarify the role of the low-speed streaks in the viscous sublayer of all turbulent wall flows by determining whether or not the polymer additives lower the drag by inhibiting the formation of these low-speed streaks. The experiments were designed to determine if the presence of a drag-reducing polymer solution in only the viscous sublayer

---

[1] Wells, C.S. and J.G. Spangler. Injection of a Drag-Reducing Fluid into Turbulent Pipe Flow of a Newtonian Fluid. The Physics of Fluids, 10, 1967, pp. 1890-1894.

[2] Wu, J. and M.P. Tulin. Drag Reduction by Ejecting Additive Solutions into Pure-Water Boundary Layer. Journal of Basic Engineering, 94, 1972, pp. 749-756.

[3] McComb, W.D. and L.H. Rabie. Development of Local Turbulent Drag Reduction Due to Nonuniform Polymer Concentration. The Physics of Fluids, 22, 1979, pp. 183-185.

of a turbulent channel flow of water would produce significant amounts of drag reduction and inhibit the formation of low-speed sublayer streaks. Consequently the experiments were designed to demonstrate whether the viscous sublayer has an active or a passive role in the production of turbulent kinetic energy.

The experiments were performed in a long water channel with a 2.5 × 25 cm rectangular cross section. Dilute polymer solutions were seeped into the viscous sublayer of the fully developed, turbulent channel flow through thin slots in both of the 25 cm walls. A fluorescent dye was added to the fluid injected through one of the slots and video recordings were made. From this flow visualization information, the transverse spacing of the low-speed streaks was measured downstream of the injection slot before the polymer could diffuse out of the sublayer. At the same time pressure drop measurements were made at several locations downstream of the injection. When these results were compared to similar pressure drop and transverse spacing measurements from experiments where both dyed water and dyed water-glycerin solutions (which matched the viscosity of the polymer solutions) were seeped into the sublayer, it was possible to deduce the effect of the polymer solution on both the structure of the viscous sublayer and the viscous wall shear stress. Thus the experimental objectives were to compare (1) the transverse spacing of the low-speed streaks and (2) the pressure drop of turbulent flows when only the viscous sublayer contains a dilute polymer solution with those same quantities when the sublayer contains Newtonian fluids. In all cases the fluid in the outer portion of the flow was water.

These comparisons indicate the lower limits of injection which can yield drag reduction and clarify the role of the viscous sublayer and the low-speed streaky structure in the production of turbulence. This is important to both our understanding of how the polymer solution directly affects the turbulent processes and of the role played by the low-speed streaks in the production of turbulent kinetic energy in Newtonian flows.

Clarification of these fundamental aspects of the physics is particularly important to analysts who are attempting to construct more general analytical models of turbulent wall flows. It should be emphasized that new models of turbulent wall flows based on the recently discovered physics

are beginning to appear in the literature [5,6,7,8,9]. None are ready for engineering calculations. Moreover, their differences emphasize the disagreement about the relative importance each analyst attaches to the various parts of the production process. However, it is the opinion of all these analysts that a model based on these physics will be more general and reliable than current turbulence models.

Relationship to other work

The experiments were directly motivated by the turbulent, wall structure studies conducted by the principal investigator at Oklahoma State University [4,10,11]. In these studies as well as those at the University

---

[4] Oldaker, D.K. and W.G. Tiederman. Spatial Structure of the Viscous Sublayer in Drag-Reducing Channel Flows. Physics of Fluids, 20, No. 10, Part II, 1977, pp. S133-S144.

[5] Orszag, S.A. Model of Burst Formation in Turbulent Boundary Layers. Proceedings of the Workshop on Coherent Structure of Turbulent Boundary Layers, Lehigh University, Bethlehem, Pennsylvania, November 1978, pp. 258-283.

[6] Doligalski, T.L. and J.D.A. Walker. Shear Layer Breakdown Due to Vortex Motion. Proceedings of the Workshop on Coherent Structure of Turbulent Boundary Layers, Lehigh University, Bethlehem, Pennsylvania, November 1978, pp. 288-332.

[7] Landahl, M.T. Modeling of Coherent Structure in Boundary Layer Turbulence. Proceedings of the Workshop on Coherent Structure of Turbulent Boundary Layers, Lehigh University, Bethlehem, Pennsylvania, November 1978, pp. 340-364.

[8] Coles, D. A Model for Flow in the Viscous Sublayer. Proceedings of the Workshop on Coherent Structure of Turbulent Boundary Layers, Lehigh University, Bethlehem, Pennsylvania, November 1978, pp. 462-475.

[9] Hatziavramidis, D.T. and T.J. Hanratty. The Representation of the Viscous Wall Region by a Regular Eddy Pattern. J. Fluid Mech., 95, 1979, pp. 655-679.

[10] Tiederman, W.G., A.J. Smith and D.K. Oldaker. Structure of the Viscous Sublayer in Drag-Reducing Channel Flows. Turbulence in Liquids 1975, ed. by J.L. Zakin and G.K. Patterson, Science Press, Princeton, New Jersey, 1977, pp. 312-322.

[11] Donohue, G.L., W.G. Tiederman and M.M. Reischman. Flow Visualization of the Near-Wall Region in a Drag-Reducing Channel Flow. J. Fluid Mech., 56, 1972, pp. 559-575.

of Illinois [12] and the University of British Columbia [13] it was shown that the nondimensional transverse spacing of the low-speed streaks within the viscous sublayer increases as the amount of drag reduction increases. These previous drag-reducing experiments were conducted with relatively dilute, homogeneous solutions of high molecular weight polymers.

This increase in the scale of the structure within the sublayer led to the hypothesis [11] that the ability of the polymer solution to resist vortex stretching could inhibit the formation of wall layer streaks. The smaller number of streaks yields a decrease in the spatially averaged bursting rate of streaks which in turn yields a decrease in turbulent transport and lower viscous drag. This explanation of how the polymer effects the turbulence was particularly attractive since two studies [10,11] showed that the time between bursts of a streak were the same for a flow of water and for a drag-reducing flow of a polymer solution at the same wall shear stress. Moreover, it was also shown [4] that at the higher values of drag reduction (above 35 to 40%), the dimensionless spacing decreases as the distances from the wall within the viscous sublayer increases. The motion pictures from this study indicated an increase in the damping of streak movement and formation as the wall is approached.

There is considerable evidence that the production of turbulent kinetic energy in a wall flow occurs in a coherent cyclic fasion [14,15,16]. This

---

[12] Eckelman, L.D., G. Fortuna and T.J. Hanratty. Drag Reduction and the the Wavelength of Flow-Oriented Wall Eddies. Nature, 236, 1972, pp. 94-96.

[13] Achia, B.U. and D.W. Thompson. Structure of the Turbulent Boundary Layer in Drag-Reducing Pipe Flow. J. Fluid Mech., 81, 1977, pp. 439-464.

[14] Willmarth, W.W. Structure of Turbulence in Boundary Layers. Advance in Applied Mechanics, Vol. 15, Academic Press, New York, NY, 1975, pp. 159-254.

[15] Structure of Turbulence and Drag Reduction. Proceedings of an International Symposium, ed. by F.N. Frenkiel, M.T. Landahl and J.L. Lumley. Physics of Fluids, 20, No. 10, Part II, 1977.

[16] Coherent Structure of Turbulent Boundary Layers. Proceedings of the Workshop, ed. by C.R. Smith and D.E. Abbott. Department of Mechanical Engineering and Mechanics, Lehigh University, Bethlehem, Pennsylvania, 1979.

quasi-periodic process consists of the penetration of high-momentum fluid into the near-wall region and the subsequent ejection of low-momentum fluid from the near-wall region. These three-dimensional sweeps of high-momentum fluid toward the wall and ejections of low-momentum fluid from the wall are separated in both space and time by relatively quiescent periods of flow where little turbulent transport occurs. Essentially all of the turbulent kinetic energy is produced and most of the turbulent transport occurs during these sweep and ejection events. Since this is a cyclic process, it is only necessary for the polymer solution to inhibit one of the events in the cycle in order to produce an effect on either all or some other aspect of the cycle. Therefore the observation of an increased spacing in a fully developed flow of a homogeneous solution does not preclude the possibility that some other feature of the cycle is directly affected by the polymer. In other words the increased spacing of the low-speed streaks may be simply the observed "symptom" and not the "direct effect" of the polymer molecules.

The other most logical process within the wall region where the polymer could directly affect the turbulent production cycle occurs in the buffer region. This is where the low-speed streaks migrate by lifting away from the wall and where they undergo a high frequency oscillation before breaking up and ejecting fluid away from the wall [17,18]. This breakup occurs at a dimensionless distance from the wall in the range $10 < y^+ < 30$. Here

$$y^+ = yv^*/\nu \qquad (1)$$

where y is the distance from the wall, ν is the kinematic viscosity of the fluid and v^* is the friction velocity given by

---

[17] Kline, S.J., W.C. Reynolds, F.A. Schraub and P.W. Runstadler. The Structure of Turbulent Boundary Layers. J. Fluid Mech., 30, 1967, pp. 741-773.

[18] Kim, H.T., S.J. Kline and W.C. Reynolds. The Production of Turbulence Near a Smooth Wall in a Turbulent Boundary Layer. J. Fluid Mech., 50, 1971, pp. 133-160.

$$v^* = \sqrt{\tau_w/\rho} \qquad (2)$$

τ_w is the wall shear stress and ρ is the density of the fluid.

Virk [19] proposed that the polymer inhibits the breakup of low-speed streaks and this was also the original hypothesis that motivated the studies at Oklahoma State. In addition Lumely believes that the polymer must have its effect in the buffer region of the flow [20]. Consequently prior to these experiments there were two hypotheses about how the polymer acts to reduce drag. One assumed that the polymer acts in a region $y^+ < 4$ to inhibit the formation of low-speed streaks. The other assumed that the polymer acts in a region $10 < y^+ < 30$ to inhibit the breakup of low-speed streaks and the subsequent ejection of low-momentum fluid. This experimental program was designed to test the relative merits of these two hypotheses.

The basic concept was to determine both the flow structure in the sublayer and the drag reduction immediately downstream of the injection of the dilute polymer solutions. The injection was controlled so that the polymer remains within the viscous sublayer for some distance. Hence immediately downstream of the slot, the only mechanism by which the polymer could effect the flow structure was by inhibiting the formation of low-speed streaks. It was some distance downstream of the slot before the polymer had diffused far enough from the wall to effect the breakup and ejection part of the cycle.

This study differs significantly in not only purpose but also plan

---

[19] Virk, P.S. Drag Reduction Fundamentals. AIChE Journal, 21, 1975, pp. 625-656.

[20] Lumley, J.L. Drag Reduction in Two Phase and Polymer Flows. The Physics of Fluids, 20, No. 10, Pt. II, 1977, pp. S64-S71.

from previous polymer injection studies [2,21,22,23,24,25,26,27] primarily because the injection flow rates were only about 1/10 the flow rate in the viscous sublayer. In contrast typically polymer solution injection rates have varied from 1 to 4 times the flow rate in the viscous sublayer [2] to much larger values [21]. It should be noted that Wu and Tulin [2] also reported some results for injection rates comparable to those of this study. The only other injection study where the flow rate was an order of magnitude lower than the flow rate in the viscous sublayer was reported by Latto and Shen [22]. However, in their study the polymer solution was injected into the laminar portion of the boundary layer. Undoubtedly the solution was well mixed with most of the boundary layer fluid downstream of the laminar to turbulent transition region. So while their polymer flow rates were quite low the polymer concentration in the turbulent boundary layer must have been relatively uniform throughout the entire layer. Our purpose of course is to have a very distinct change from a dilute polymer solution well

[21] Fruman, D.H. and M.P. Tulin. Diffusion of a Tangential Drag Reducing Polymer Injection on a Flat Plate at High Reynolds Numbers. J. of Ship Research, 20, 1976, pp. 171-180.

[22] Latto, Brian and Chi-Hung Shen. Experimental Investigation of Polymer Solution Injection on External Boundary Layers. Proceedings of the Symposium on Turbulence Measurements in Liquids, September 1969 edited by G.K. Patterson and J.L. Zakin, Dept. of Chemical Engrg., University of Missouri-Rolla, 1971, pp. 110-115.

[23] Tullis, J.P. and K.L.V. Ramu. Drag Reduction in Developing Pipe Flow with Polymer Injection. BHRA International Conference on Drag Reduction, Sept., 1974, Paper G3.

[24] Latto, Brain and O.K.F. ElRiedy. Diffusion of Polymer Additives in a Developing Turbulent Boundary Layer. J. Hydronautics, 10, 1976, pp. 135-139.

[25] Wu, J., D.H. Fruman and M.P. Tulin. Drag Reduction by Polymer Diffusion at High Reynolds Numbers. J. Hydronautics, 12, 1978, pp. 134-136.

[26] Fruman, D.H. and P. Galivel. Near-Field Viscoelastic Effects During Thin-Slit Drag-Reducing Polymer Injection. Journal of Rheology, 24, 1980, pp. 627-646.

[27] Fruman, D.H. and P. Galivel. Anomalous Effects Associated with Drag-Reducing Polymer Ejection into Pure-Water Turbulent Boundary Layers. Viscous Flow Drag Reduction, Vol. 72, Progress in Astronautics and Aeronautics, ed. by G.R. Hough. American Institute of Aeronautics and Astronautics, New York, NY, 1980, pp. 332-350.

within the viscous sublayer to pure water in the remainder of the flow.

Several times the term "dilute solution" has been used to denote solutions whose concentrations are on the order of hundred parts per million or less. At these relatively low concentrations the viscosity of the solution is similar to the viscosity of water. This distinction is made because there have been studies where concentrated solutions ($\sim$ 5000 ppm) with much higher viscosities than water have been injected into water [28,29,30]. In these studies, the highly concentrated polymer solution neither dissolved in nor mixed well with the water. Thus, downstream of injection the flows contained threads of concentrated polymer solution more or less dispersed in at least the outer regions of tube flows. The relationship of these works to this study is not completely clear. However, one would suspect that the drag reduction achieved was due to an entirely different mechanism than that which occurs with a dilute solution.

There is of course a strong coupling or interaction between the flow in the outer portion of a boundary layer or the center portion of a tube and the flow in the near-wall region [31,32,33]. It is not the intention

---

[28] Vleggaar, J. and M. Tels. Drag Reduction by Polymer Threads. Chemical Engineering Sci., 28, 1973, pp. 965-968.

[29] Stenberg, L.-G., T. Lagerstedt, O. Sehlén and E.R. Lindgren. Mechanical Mixing of Polymer Additive in Turbulent Drag Reduction. The Physics of Fluids, 20, 1977, pp. 858-859.

[30] Stenberg, L.-G., T. Lagerstedt and E.R. Lindgren. Polymer Additive Mixing and Turbulent Drag Reduction. The Physics of Fluids, 20, No. 10, Pt. II, 1977, pp. S276-S279.

[31] Offen, G.R. and S.J. Kline. Combined Dye-Streak and Hydrogen-Bubble Visual Observations of a Turbulent Boundary Layer. J. Fluid Mech., 62, 1974, pp. 223-240.

[32] Praturi, A.K. and R.S. Brodkey. A Stereoscopic Visual Study of Coherent Structures in Turbulent Shear Flow. J. Fluid Mech., 89, 1978, pp. 251-272.

[33] Smith, C.R. Visualization of Turbulent Boundary-Layer Structure Using a Moving Hydrogen Bubble-Wire Probe. Proceedings of the Workshop on Coherent Structure of Turbulent Boundary Layers, Lehigh University, Bethlehem, Pennsylvania, November 1978, pp. 48-94.

of this program to study this interaction directly. However the study does fit into the overall scheme of coherent structure studies including those boundary layer experiments that focus on the structures in the outer portion of the flow [34,35].

---

[34] Nychas, S.G., H.C. Hershey and R.S. Brodkey. A Visual Study of Turbulent Shear Flow. J. Fluid Mech., 61, 1973, pp. 513-540.

[35] Falco, R.E. Coherent Motions in the Outer Region of Turbulent Boundary Layers. Physics of Fluids, 20, No. 10, Part II, 1977, S124-S132.

EXPERIMENTAL APPARATUS AND PROCEDURES

The experiments were conducted in the flow loop shown in Figure 1. Water is circulated by centrifugal pumps whose flow rate is measured by a 1.812-inch, sharp edged orifice located in a 21/2-inch PVC pipe. Fluid enters the upstream stilling chamber through a 4-inch PVC pipe which extends from the bottom of the chamber to near the top. This pipe is capped at the top and uniformly perforated with 1/2-inch holes that initially distribute the incoming flow. A perforated plate and a screen-sponge-screen section separate the inlet of the upstream chamber from its outlet. The outlet is a smooth two-dimensional contraction from the 60 x 60 cm cross section of the upstream chamber to the 2.5 x 25 cm cross section of the channel. Immediately downstream of this contraction is a flow straightener composed of plastic drinking straws. Consequently the flow enters the test section without any large scale vorticity.

At the downstream end of the test section, a large stilling tank ensures that disturbances from the outlet are not transmitted upstream. Located in this downstream tank is a cooling coil which yields excellent temperature control during an extended test. The two stilling tanks as well as the test section were constructed from 1/2-inch plexiglas sheet.

The internal dimensions of the test section's rectangular cross section are 2.5 x 25 cm or 0.980 x 9.84 inches which gives the channel an aspect ratio of 10 to 1. The injection slots are located 63 channel widths downstream of the channel entrance and 34 channel widths upstream of the exit. Consequently the flow in the region of the injection slots is typical of fully developed, two-dimensional channel flow.

The injected fluid flows by gravity from reservoirs above the channel, through Gilmont rotameter flow meters and flow control valves to the two injection slots. As shown in Figure 1, a separate system supplied fluid to slots in each of the 25 cm walls of the channel. Clear fluid was supplied to the slot in the top wall while dyed fluid used for flow visualization was piped to the bottom slot. The rotameters were calibrated for each fluid that was injected.

As shown in Figure 2, each slot was 0.005 inches wide, 8.84 inches long and centered in the 10.84 inch section that formed the 25 cm walls of the

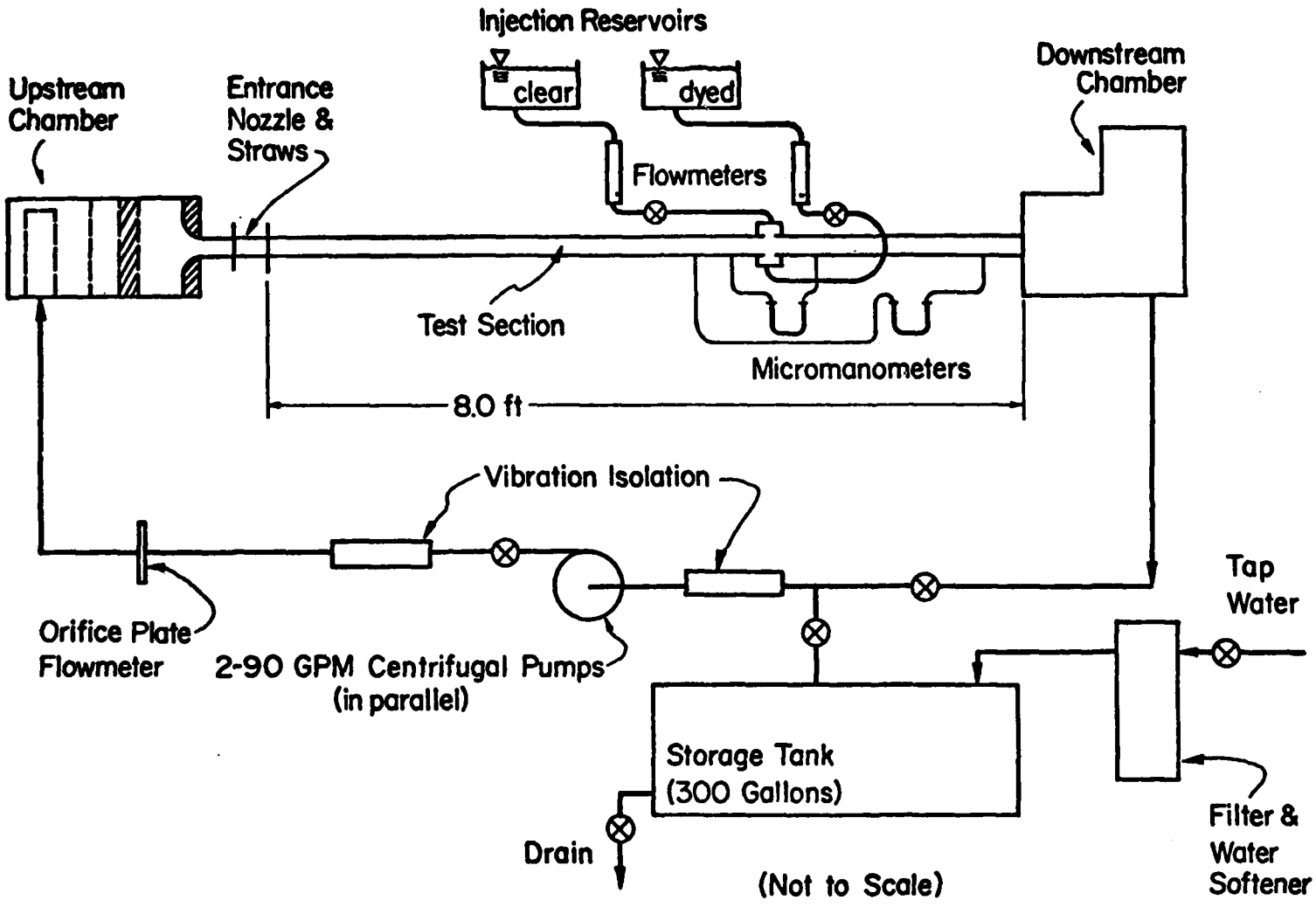

Figure 1. Schematic of flow loop.

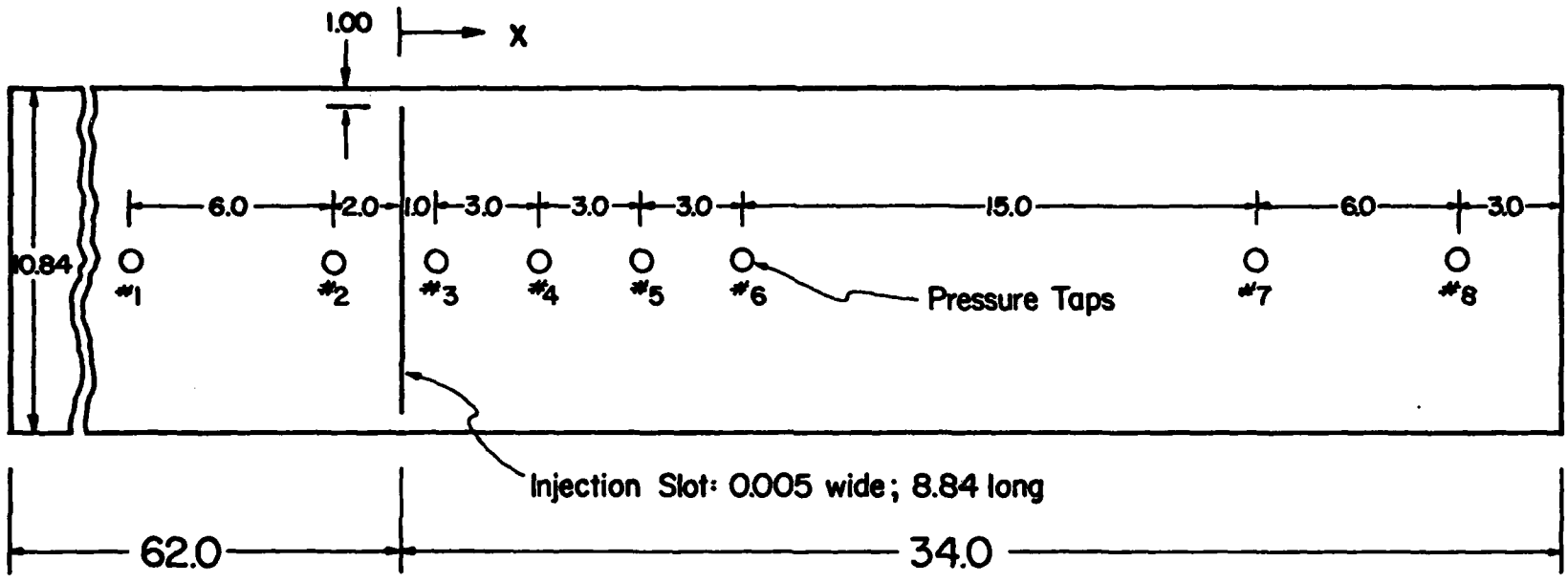

Figure 2. Schematic of bottom wall showing location of injection slot and pressure taps.

test section. As a result fluid was not injected into either the corners or along the 2.5 cm side walls of the channel.

Also shown in Figure 2 are the streamwise locations of the pressure taps that were centered in the bottom wall of the channel. Tap number 1 is 8 inches upstream of the injection slots and tap number 8 is 31 inches downstream of the slots. Of course the most critical taps are those which are nearest the injection. Each static pressure hole has a diameter of 1/16 inch and a length of 1/8 inch which connects the tap to a 1/4-inch tube glued into the outside of the plastic wall. All holes were drilled carefully to ensure that they are perpendicular with the surface and free of burrs and chips.

Two Gilmont micrometer manometers with carbontetrachloride as the manometer fluid were used to measure the pressure drop. With this manometer fluid the pressure measurements could be made with a sensitivity of 1.5×10^{-2} mm or 6×10^{-4} inches of water.

The lighting and camera configuration used to obtain motion pictures of the sublayer streaks is shown in Figure 3. The camera and strobe light are components of a Video Logic Corporation INSTAR IV high-speed motion analyzer system. The strobe gives the camera an effective exposure time of 10 microseconds while the camera produces 120 pictures per second that are recorded on one-inch video tape. Using the front-surface mirror shown in Figure 3, the camera produces a plan view of the fluorescent dye marked streaks on the bottom wall. The line of sight is through the clear fluid injected through the top wall which is necessary to produce a symmetric flow field and to yield a measurable drag reduction. Further discussion of this fluorescent dye visualization technique can be found in Reference [4].

The fluorescent fluid was a 4 gram per liter concentration of Fluorescein disodium salt. The fluids injected into the water flows were water, a 100 ppm solution of SEPARAN AP-273, a 400 ppm solution of AP-273, and two mixtures of glycerin and water that matched the viscosity of the two polymer solutions. Viscosities of all injected fluids, both clear and dyed, were measured with LVT-SCP Wells-Brookfield, 1.565° cone and plate, micro viscometer at shear rates of 115 and 230 sec^{-1}.

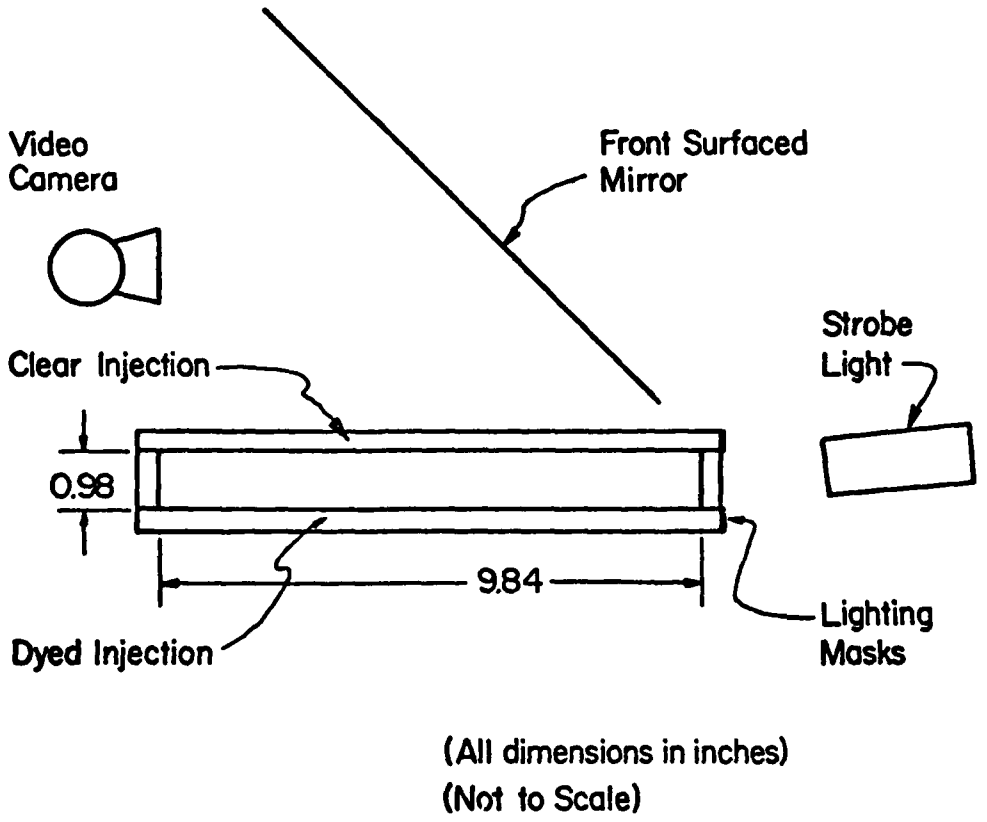

Figure 3. Lighting and camera arrangement.

The drag reducing capability of the polymer solutions both with and without dye were measured in a separate, horizontal 5/8-inch O.D. (0.553 inch I.D.) tube. The tube was gravity fed from an upstream reservoir while the flow rate was controlled by a valve at the tube's outlet. The flow rate was measured by timing the collection of a fixed mass of fluid while the pressure drop from two taps separated by 78 3/4 inches was measured with an inverted U-tube manometer. The upstream pressure tap was 20 inches from the entrance of the tube and the downstream tap was 10 inches upstream of the exit.

Procedures

One of the initial tasks of each experiment was preparation of the micromanometers. The key element in this preparation was a cleaning procedure (see Appendix A for details) that included chromic acid soaks and multiple flushes with alcohol and deionized water. When a manometer was sufficiently clean, it would yield accurate results for several days. When not properly cleaned, the meniscus between the water and carbontetrachloride would stick to the glass and/or become contaminated. In either case the resulting measurements would be neither reproducible nor accurate. It should be emphasized that using deionized water above the carbontetrachloride contributed significantly to the duration of a noncontaminated and stable interface.

The specific gravity, S.G., of carbontetrachloride at room temperature is 1.591. Consequently the relationship between the pressure drop, ΔP, and the manometer deflection, h, is given by

$$\Delta P = \rho(S.G. - 1)gh \qquad (3)$$

where ρ is the density of water and g is the acceleration of gravity.

Tap water for the main channel flow passed through a filter and a Calgon water softener prior to entering the storage tank for the flow loop. It was de-aerated by heating to about 105°F and then cooled to room temperature before being circulated in the flow loop.

The polymer solutions and glycerin mixtures were made with filtered tap water. The water used for the polymer solutions was boiled and then cooled prior to adding the polymer (see Appendix B for details). These polymer solutions initially were mixed to produce concentrations of 800 and 2560 ppm.

These concentrated mixtures were allowed to hydrate for 12 to 24 hours prior to dilution to 100 and 400 ppm respectively. The quantity of polymer solution prepared in each batch was sufficient to conduct both the drag reduction tests in the 5/8-inch tube and the channel injection experiments.

The basic plan for each experiment was to measure the pressure drop between various taps both with and without injection and to make a video tape of the streaks. All of this was done at a constant channel flow rate of 64 GPM. Usually two pressure measurements (two manometers) were made during the flow visualization with the remainder of the pressure drop measurements following after the flow visualization was completed.

Several comments are in order regarding the flow condition chosen for the comparisons. Flow visualization and accurate pressure measurements impose opposite demands upon an experiment. The best flow visualization can be accomplished at low flow rates where the pressure drop is difficult to measure. Conversely if the flow rate is higher, the pressure drop measurement is easier and the flow visualization is more difficult. After conducting a series of preliminary experiments it became clear that a comprehensive and unequivocal set of pressure drop measurements would require a relatively high flow rate. Fortunately close up lenses and the sharp image resulting from the 10 microsecond exposure made resolution of as many as 12 or so streaks per inch possible. By pushing the flow rate to a level near the limits of our current flow visualization capability it was possible to meet these two opposite demands at a rate of 64 GPM. At this flow, the Reynolds number based upon the mass average velocity, hydraulic diameter and viscosity of water at 74°F was 31,600, the shear velocity was 0.0368 m/s (0.12 ft/sec) and the shear rate at the wall with water as the fluid was 1450 sec^{-1}.

Since the viscosity of dilute polymer solutions varies with shear rate, determination of the viscosities of injected polymer solutions required estimates of the shear rate in the wall region. By assuming that the wall shear stress, τ_w, was approximately the same as the water value and that the viscosity, μ, was approximately equal to the value measured at 230 sec^{-1}, the shear rate at the wall, dU/dy) was estimated as:

$$\left.\frac{dU}{dy}\right|_o = \frac{\tau_w}{\mu} \qquad (4)$$

The viscosities of the polymer solutions were measured with a viscometer at shear rates of 115 and 230 sec^{-1}. Since the estimated shear rates in the wall region were greater than 230 sec^{-1}, an extrapolation of the measured viscosities was calculated based on the following relationship that experimentally was demonstrated by Oldaker [36]:

$$\log_{10}(\mu) = A - B \log_{10}\left(\frac{dU}{dy}\right) \qquad (5)$$

Here A and B are constants. As will be seen later, the conclusions are not effected by these approximations.

It should be noted that plexiglas absorbs water and this will cause an unconstrained edge to warp slightly. Since the geometric changes are small, they normally do not have a significant effect on the flow. However a small deflection of a few thousands of an inch at the injection slots did have a measureable effect on the reading of pressure tap number 3. This was minimized by carefully checking the channel for flattness with a long straight edge and by providing additional physical constraint in this region with a large "C" clamp when necessary.

---

[36] Oldaker, D.K. An Experimental Investigation of the Near-Wall Flow Structure During Drag Reduction. M.S. thesis, Oklahoma State University, Stillwater, Oklahoma, December, 1974.

EXPERIMENTAL RESULTS

Experimental Conditions

A summary of the experimental conditions is given in Table 1. The injection rate of 40 mℓ/min is the flow rate through each slot. This injection rate corresponds to 1/10 of the flow rate past the transverse extent of the slot and between $0 \leq y^+ \leq 8$. This is essentially 1/10 of the flow rate in the undisturbed viscous sublayer over each slot. At this and lower flow rates, the injected fluid turns when it exits the slot and flows along the surface without jetting away from the surface.

TABLE 1. Experimental Conditions

Experiment number	Injected fluid	Channel flow rate (GPM)	Injection flow rate (mℓ/min)	Kinematic viscosity of water $\nu \times 10^6$ (m^2/s)	Kinematic viscosity of injection $\nu \times 10^6$ (m^2/s)
935	AP-273 100 ppm	64	40	0.893	1.36*
940 945	AP-273 400ppm	64	40	0.905	2.75*
950 955	Glycerin 36%	64	40	0.928	2.90 2.73
960	AP-273 100 ppm	64	40	0.926	1.28*
970	Glycerin 16%	64	40	0.916	1.38
980	Water	64	40	0.916	0.916

*Extrapolated values for the estimated shear rate.

Demonstration of drag reduction in 5/8-inch tube

There were two objectives for the drag reduction tests conducted in the 5/8-inch tube. The first was to verify that the fluorescent dye did not degrade the drag reducing capability of the polymer solution. The second was to verify that the polymer injected into the channel was in fact capable of producing drag reduction.

A series of experiments showed that the skin friction coefficient, c_f, for water flowing in the tube was given by

$$c_f = 0.079\ Re^{-1/4} \tag{6}$$

The skin friction coefficient is defined by

$$c_f = \frac{\tau_w}{\frac{1}{2}\rho U^2} \tag{7}$$

and the Reynolds number, Re, is

$$Re = \frac{UD}{\nu} \tag{8}$$

where ρ is the density of the fluid, U is the mass average velocity and D is the internal diameter of the tube. Since the flow in the section between the pressure taps is fully developed, the pressure gradient, $\Delta P/\Delta x$, and wall shear stress are realted by

$$\frac{\Delta P}{\Delta x} = \tau_w\ (4/D) \tag{9}$$

For the polymer solutions, percent drag reduction, DR, was defined by the equation

$$DR = 100((c_f)_w - (c_f)_p)/(c_f)_w) \tag{10}$$

where $(c_f)_p$ is the skin friction coefficient for the polymer solution and $(c_f)_w$ is the skin friction coefficient for a water flow that has the same flow rate as the polymer solution. The latter is calculated using Equation 6 and water properties to evaluate the Reynolds number.

Results for the experiments with SEPARAN AP-273 solutions are plotted in Figure 4. The open symbols for the 100 ppm solutions were experiments with a batch of polymer none of which was injected into the channel while the closed symbols are for a portion of the polymer batches used in channel flow experiments number 935 and 960. Similarly portions of the 400 ppm solutions shown on Figure 4 were used as the injected fluids in experiment number 940.

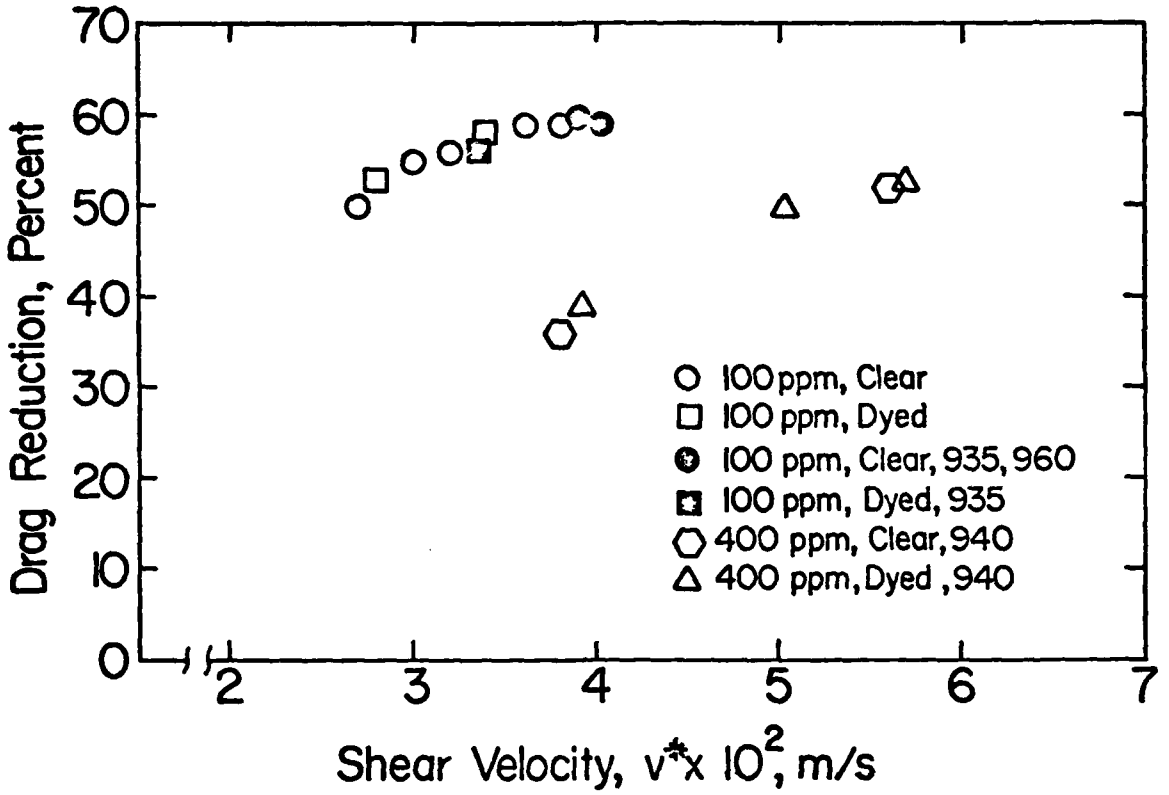

Figure 4. Demonstration of drag-reducing capability of polymer solutions in a 5/8-inch tube.

As these results clearly show, the dye did not effect the drag reducing capability of the polymer solutions. All solutions used in the channel flow experiments were capable of producing drag reduction and the 100 ppm results indicate that there was reasonable uniformity in the quality of the solutions from batch to batch.

The 400 ppm results fall below the 100 ppm results due to the higher viscosity of the more concentrated solution. For example, at a shear velocity of 0.037 m/s the 36% drag reduction achieved in the tube almost corresponds to a laminar friction coefficient for a 3 centipoise Newtorian fluid.

Pressure drop comparisons in the channel

As might be expected, the pressure differences in the immediate vicinity of the injection slots were those that were effected most by the injection of a fluid. The results shown in Table 2 for the injection of water are typical of the results for the injection of Newtonian fluids. Tap

number 2 is 2.0 inches upstream of the slots and tap number 3 is 1.0 inches downstream. Consequently the small negative drag reduction, which

TABLE 2. Pressure Drop Results for Water Injection, Experiment 980

Pressure taps	Distance between taps (inches)	Average Streamwise location (inches)	Manometer deflections No injection h (inches×10^3)	Injection h_i (inches×10^3)	$h-h_i$ (inches×10^3)	Drag reduction (%)
2-3	3.0	-0.5	44	45	-1	-2
3-4	3.0	2.5	58	58	0	0

corresponds to a slight increase in the pressure drop between taps 2 and 3, occurs because the injected fluid must acquire streamwise momentum. Recall that the slot itself is perpendicular to the flow direction. Pressure tap 4 is 4 inches downstream of the slots. Hence the comparison between no injection and injection for the pressure difference between taps 3 and 4 indicates that the injection is no longer having a measurable influence on the local friction for $x \geq 1.0$ inch. The streamwise location, x, is measured from the injection slots. Positive values of x correspond to a downstream while negative values correspond to an upstream location with respect to the slots.

The pressure drop comparison for the injection of a 100 ppm solution of AP-273 appear in Table 3 and Figure 5. Also shown on Figure 5 and in Table 4 are the results obtained when a 16% glycerin solution was injected through the slots. This glycerin solution had essentially the same viscosity as the 100 ppm polymer solution.

Figure 6 gives a comparison between the pressure drop measurements for the 400 ppm AP-273 injection and the 36% glycerin injection. Notice that there is also a limited comparison for the case where the 400 ppm solution is injected through only one slot. The data for the 400 ppm polymer solutions is shown in Table 5 while Table 6 contains the data for the 2.70 centipoise 36% glycerin injection.

TABLE 3. Pressure Drop Results for 100 ppm AP-273 injection, Experiment 960

Pressure taps	Distance between taps (inches)	Average Streamwise location (inches)	Manometer deflections No injection h (inches×10^3)	Injection h_i (inches×10^3)	$h-h_i$ (inches×10^3)	Drag reduction (%)
1-2	6.0	-5.0	117	117	0	0
2-3	3.0	-0.5	38	41	-3	-8
3-4	3.0	2.5	59	58	1	2
4-5	3.0	5.5	62	52	10	16
5-6	3.0	8.5	45	40	5	11
6-7	15.0	17.5	262	248	14	5
7-8	6.0	28.0	110	106	4	4
1-8	39.0	11.5	732	707	15	2

TABLE 4. Pressure Drop Results for 16% Glycerin Injection, Experiment 970

Pressure taps	Distance between taps (inches)	Average Streamwise location (inches)	Manometer deflections No injection h (inches×10^3)	Injection h_i (inches×10^3)	$h-h_i$ (inches×10^3)	Drag reduction (%)
2-3	3.0	-0.5	40	43	-3	-8
3-4	3.0	2.5	56	56	0	0
4-5	3.0	5.5	62	62	0	0
5-6	3.0	8.5	49	49	0	0
6-7	15.0	17.5	266	266	0	0
1-8	39.0	11.5	733	736	-3	-0.4

In all cases the basis for calculating the amount of drag reduction was the pressure drop when no injection was occurring. Recall there is effectively no difference in the pressure drop between the cases of no injection and water injection.

Obviously there is a continuous variation of skin friction. However, since the pressure taps are separated by three or more inches, the data only yields the average pressure drop over the distance between the taps.

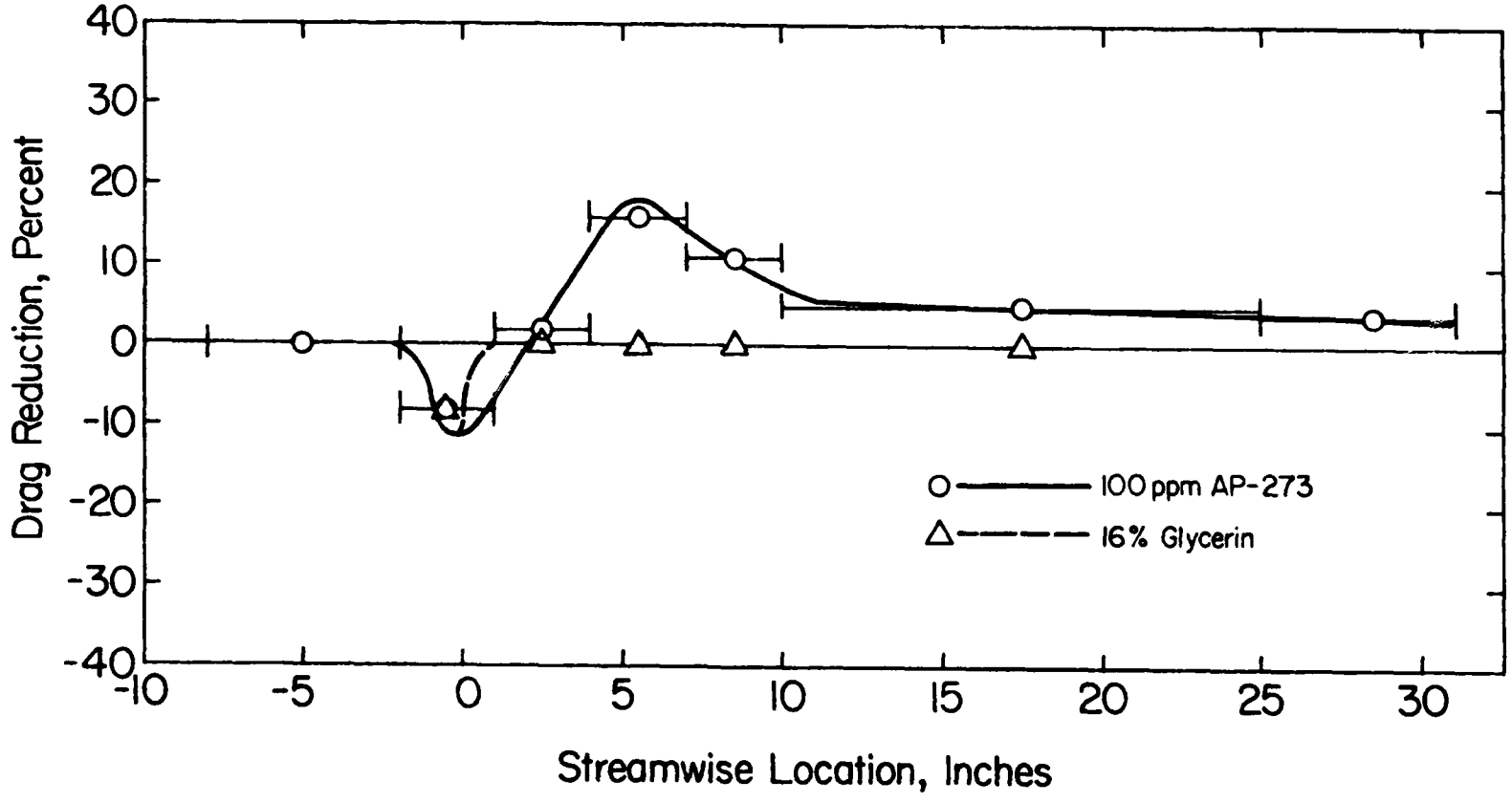

Figure 5. Drag reduction results for the injection of a 100 ppm solution of AP-273 and 16% glycerin solution into the channel flow of water.

TABLE 5. Pressure Drop Results for 400 ppm AP-273 Injection, Experiments 940;945

Pressure taps	Distance between taps (inches)	Average Streamwise location (inches)	Manometer deflections No injection h (inches×10^3)	Injection h_i (inches×10^3	$h-h_i$ (inches×10^3)	Drag reduction (%)
			Injection through both slots			
1-2	6.0	-5.0	111	111	0	0
2-3	3.0	-0.5	32	41	-9	-28
3-4	3.0	2.5	60	63	-3	-5
4-5	3.0	5.5	67	49	18	27
5-6	3.0	8.5	49	38	11	22
7-8	6.0	28.0	118	105	13	11
1-8	39.0	11.5	724	648	76	10
1-8	39.0	11.5	722	653	69	10
			Injection through only the top slot			
1-2	6.0	-5.0	111	111	0	0
2-3	3.0	-0.5	32	38	-6	-19
3-4	3.0	2.5	60	62	-2	-3
4-5	3.0	5.5	67	62	5	7
7-8	6.0	28.0	118	111	7	6
1-8	39.0	11.5	724	684	40	6
1-8	39.0	11.5	722	685	37	5

TABLE 6. Pressure Drop Results for 36% Glycerin Injection, Experiment 955

Pressure taps	Distance between taps (inches)	Average Streamwise location (inches)	Manometer deflections No injection h (inches×10^3)	Injection h_i (inches×10^3)	$h-h_i$ (inches×10^3)	Drag reduction (%)
1-2	6.0	-5.0	120	120	0	0
2-3	3.0	-0.5	39	42	-3	-8
3-4	3.0	2.5	61	61	0	0
4-5	3.0	5.5	58	58	0	0
6-7	15.0	17.5	252	252	0	0
7-8	6.0	28.0	107	107	0	0
1-8	39.0	11.5	733	737	-4	-0.5
1-8	39.0	11.5	728	732	-4	-0.5

This is shown by plotting the data point at the center or average location and by showing the Δx associated with that measurement by a horizontal line with short vertical bars at its ends. The position of the continuous lines drawn through the data was then estimated such that the area "under" the continuous curve is about the same as the area under the horizontal line through the data point.

For all cases where a polymer solution was injected, there is a significant drag increase in the immediate vicinity of the slot. Notice that this drag increase for the 100 ppm solution is almost the same as the increase for the 16% glycerin injection. However, the drag increase for the 400 ppm polymer solution is significantly greater than the increase for the 36% glycerin solution. Neither glycerin solution showed any evidence of drag reduction. However, as in the case of water, the injection of these glycerin solutions does not effect the pressure drop for $x \geq 1.0$ inch.

A best estimate for the onset of drag reduction for the 100 ppm solution of AP-273 is $x = 2.0$ inches. This corresponds to a dimensionless value of $x^+ = xv^*/\nu = 2000$. For the 400 ppm solution, drag reduction appears to begin at $x = 3.0$ inches or $x^+ = 3100$. Here an average shear velocity based on all the experiments of 0.0368 m/s was used to calculate x^+ while ν was the kinematic viscosity of the water for that particular experiment.

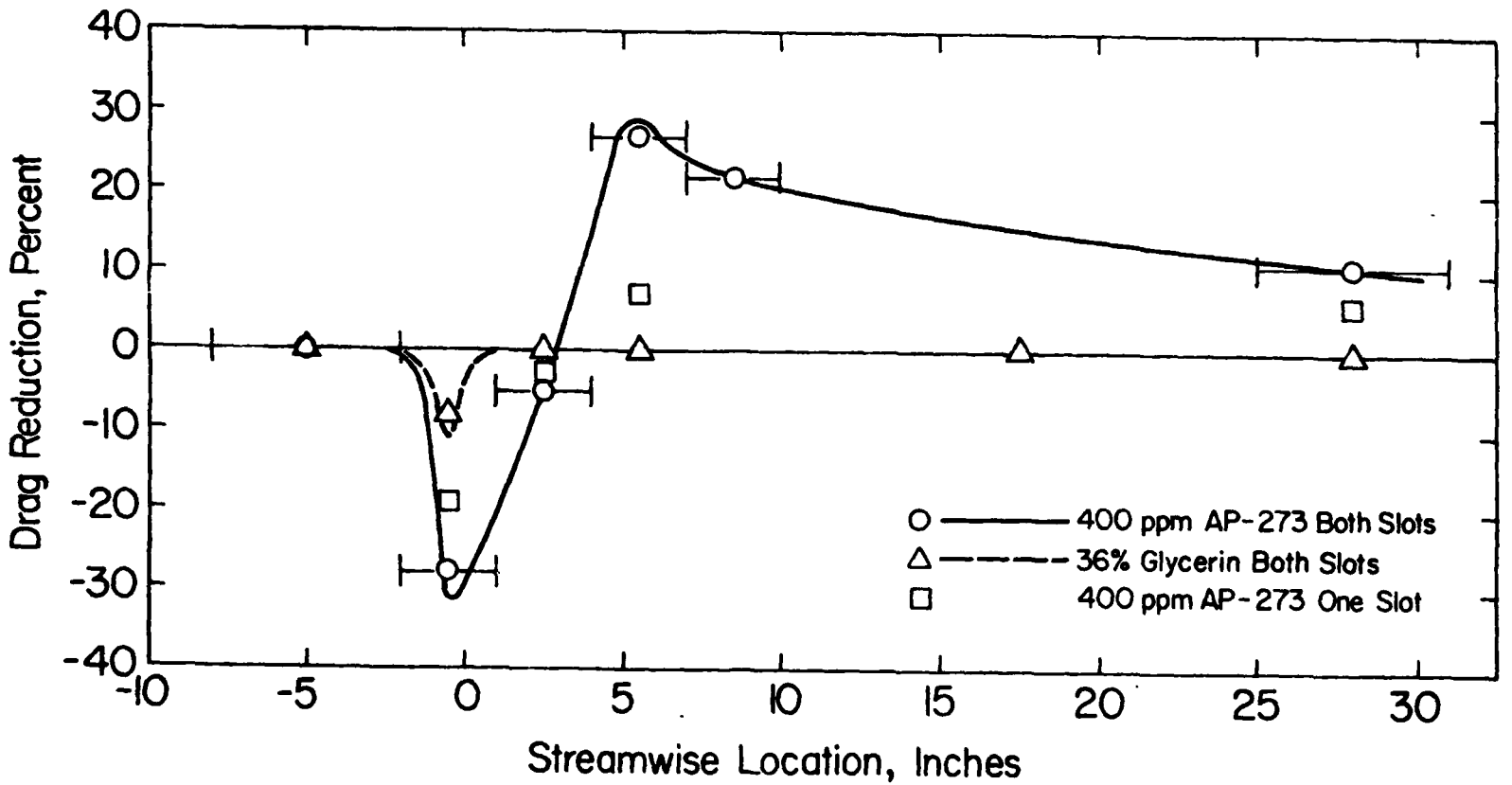

Figure 6. Drag reduction results for the injection of a 400 ppm solution of AP-273 and a 36% glycerin solution into the channel flow of water.

In all drag-reducing cases, the amount of drag reduction slowly decreases after reaching a peak 5 1/2 inches downstream of the slots. The slow decrease is most likely due to a decrease in polymer concentration in the wall region. These injection experiments were not too effective at producing drag reduction. These results and others [2,4] would indicate that more polymer molecules were needed.

Streak spacing

The techniques used for deducing the spanwise spacing between the streaks from the video tapes were based upon the methods described by Oldaker and Tiederman [4]. The basic idea involves counting the number of streaks in about fifteen statistically independent frames of the video tape and then calculating the average spanwise spacing $\overline{\lambda}$, from

$$\overline{\lambda} = b/\overline{N}$$

Here b is a spanwise distance marked on a transparent overlay, placed on the video screen that correspond to 25 mm in the flow; $\overline{N}$ is the average number of streaks per frame.

Consistent with Reference 4 a streak was defined to be a clearly identifiable single longitudinal structure that has a streamwise length of at least four times the apparent average spanwise spacing between streaks. Streaks were counted at downstream locations identified by a line on the overlay for the video screen that was parallel to the injection slots.

Four observors counted streaks for each of the results given in Table 7. Each observor sat about 1 m in front of the screen and viewed the video tapes at a speed that was 3% of the recording speed. The tape was stopped at approximately equal intervals of time and streaks were counted. The average number of streaks per frame was calculated for each observor and the mean of these averages was used to determine $\overline{N}$ and $\overline{\lambda}$. The dimensionless location for these counts as well as the dimensionless spacing $\lambda^+ = \overline{\lambda}v^*/\nu$ are shown in Table 7.

The obvious result clearly shown in Table 7 is that the streak spacing when non-dimensionalized with the viscosity of water was the same for all injected fluids. The value of $\lambda^+ \sim 100$ is the often quoted result for water.

TABLE 7. Summary of Streak Spacing Results

Experiment	Scene	Injected fluid	Dimensionless streamwise location x^+	Average[a] number of streaks $\overline{N}$	Average spanwise spacing $\overline{\lambda}$ (mm)	Dimensionless spacing λ^+
980	981	Water	502	9.58	2.61	105
980	982	Water	301	9.41	2.66	107
935	936	100 ppm AP-273	515	9.69	2.58	106
970	971	16% glycerin	502	9.94	2.52	101
970	972	16% glycerin	301	9.92	2.52	101
940	941	400 ppm AP-273	508	10.28	2.43	99
950	951	36% glycerin	496	9.84	2.54	101

[a]Average from four independent observers who counted streaks over a spanwise distance of 25 mm.

This is significantly lower than the value of $\lambda^+ \sim 200$ that was obtained in a similar flow where all of the fluid was a homogeneous, 100 ppm solution of AP-273 [4].

The final result is an observation from the flow visualization. In the plan view of the streaks, it is possible to make rough estimates of the streak length by noting the average location where the streaks begin to mix with fluid further from the wall. For the two experiments where the injected fluid was a glycerin solution and for the water injection experiment the streak length, ℓ, was one inch or less ($\ell^+ \lesssim 1000$). When 100 ppm of AP-273 was injected, there seemed to be slightly less mixing and the streak length was about one inch. However, for the 400 ppm injection, the streak length was three or more inches ($\ell^+ \sim 3000$) and there was considerably less mixing between the sublayer and the rest of the flow. In spite of these observations regarding streak length, it should be noted again that the peak drag reduction for both the 100 ppm and the 400 ppm solution occurred at essentially the same downstream location of 5 1/2 inches.

CONCLUSIONS

Both the flow visualization and the pressure drop results demonstrate that a thin region of drag-reducing polymer solution within only the viscous sublayer is not capable of either modifying the spanwise spacing of the sublayer streaks or lowering the viscous drag. Drag reduction begins only after there has been some mixing of the injected fluid with the outer portion of the flow. Consequently it appears that the polymer has a direct effect on the flow in the buffer region where $10 < y^+ < 30$.

Nonetheless the increased length of the streaks in the 400 ppm injection experiments suggests that two time scales are the involved in the transport of fluid from the layers adjacent to the wall. One time scale is associated with transport from $y^+ = 0$ to $y^+ = 10$ or so. The second time scale is the bursting period or the time between bursts which transport momentum and mass from $y^+ \sim 10$ to 15 to the central portion of the channel. This conclusion is consistent with the clear demonstration that the streaks must travel some distance downstream within the sublayer before marked fluid reaches a height from which it can be involved in an ejection or burst [10,37].

The much larger drag increase of the 400 ppm polymer solution in the vicinity of the slot compared to the glycerin solution with the same viscosity indicates an anomalous effect that does not appear to be present in the 100 ppm injection. The effect may be due to swelling of the polymer solution as it exists the slot [27]. However, side-view visualization that would confirm this conclusion was not conducted.

---

[37] Bogard, D.G. and W.G. Tiederman. Investigation of Flow Visualization Techniques for Detecting Turbulent Bursts. Paper presented at the Seventh biennial symposium on turbulence, University of Missouri-Rolla, September, 1981.

RECOMMENDATIONS

Future investigations that are concerned with the mechanisms by which long-chain polymer molecules reduce drag should concentrate on the flow structures and interactions in the buffer region of the flow. In particular it would be appropriate to look again at the bursting rate of streaks in drag-reducing flows. Recall that the ejection or burst takes place in a region that is above the viscous sublayer.

Side-view flow visualization is also recommended to determine precisely the differences in migration of the various solutions from the sublayer to the buffer region and to determine if the more concentrated solutions swell as they leave the slot.

Clearly an injection scheme that optimizes drag reduction should put drag-reducing solutions into the buffer region of the flow as quickly as possible. This would appear to require injection flow rates on the order of the sublayer flow rate at least at the upstream location of injection.

REFERENCES

1. Wells, C.S. and J.G. Spangler. Injection of a Drag-Reducing Fluid into Turbulent Pipe Flow of a Newtonian Fluid. The Physics of Fluids, 10, 1967, pp. 1890-1894.

2. Wu, J. and M.P. Tulin. Drag Reduction by Ejecting Additive Solutions into Pure-Water Boundary Layer. Journal of Basic Engineering, 94, 1972, pp. 749-756.

3. McComb, W.D. and L.H. Rabie. Development of Local Turbulent Drag Reduction Due to Nonuniform Polymer Concentration. The Physics of Fluids, 22, 1979, pp. 183-185.

4. Oldaker, D.K. and W.G. Tiederman. Spatial Structure of the Viscous Sublayer in Drag-Reducing Channel Flows. Physics of Fluids, 20, No. 10, Part II, 1977, pp. S133-S144.

5. Orszag, S.A. Model of Burst Formation in Turbulent Boundary Layers. Proceedings of the Workshop on Coherent Structure of Turbulent Boundary Layers, Lehigh University, Bethlehem, Pennsylvania, November 1978, pp. 258-283.

6. Doligalski, T.L. and J.D.A. Walker. Shear Layer Breakdown Due to Vortex Motion. Proceedings of the Workshop on Coherent Structure of Turbulent Boundary Layers, Lehigh University, Bethlehem, Pennsylvania, November1978, pp. 288-332.

7. Landahl, M.T. Modeling of Coherent Structure in Boundary Layer Turbulence. Proceedings of the Workshop on Coherent Structure of Turbulent Boundary Layers, Lehigh University, Bethlehem, Pennsylvania, November 1978, pp. 340-364.

8. Coles, D. A Model for Flow in the Viscous Sublayer. Proceedings of the Workshop on Coherent STructure of Turbulent Boundary Layers, Lehigh University, Bethlehem, Pennsylvania, November 1978, pp. 462-475.

9. Hatziavramidis, D.T. and T.J. Hanratty. The Representation of the Viscous Wall Region by a Regular Eddy Pattern. J. Fluid Mech., 95, 1979, pp. 655-679.

10. Tiederman, W.G., A.J. Smith and D.K. Oldaker. Structure of the Viscous Sublayer in Drag-Reducing Channel Flows. Turbulence in Liquids 1975, ed. by J.L. Zakin and G.K. Patterons, Science Press, Princeton, New Jersey, 1977, pp. 312-322.

11. Donohue, G.L., W.G. Tiederman and M.M. Reischman. Flow Visualization of the Near-Wall Region in a Drag-Reducing Channel Flow. J. Fluid Mech., 56, 1972, pp. 559-575.

12. Eckelman, L.D., G. Fortuna and T.J. Hanratty. Drag Reduction and the Wavelength of Flow-Oriented Wall Eddies. Nature, 236, 1972, pp. 94-96.

13. Achia, B.U. and D.W. Thompson. Structure of the Turbulent Boundary Layer in Drag-Reducing Pipe Flow. J. Fluid Mech., 81, 1977, pp. 439-464.

14. Willmarth, W.W. Structure of Turbulence in Boundary Layers. Advance in Applied Mechanics, Vol. 15, Academic Press, New York, NY, pp. 159-254.

15. Structure of Turbulence and Drag Reduction. Proceedings of an International Symposium, ed. by F.N. Frenkiel, M.T. Landahl and J.L. Lumley. Physics of Fluids, 20, No. 10, Part II, 1977.

16. Coherent Structure of Turbulent Boundary Layers. Proceedings of the Workshop, ed. by C.R. Smith and D.E. Abbott. Department of Mechanical Engineering and Mechanics, Lehigh University, Bethlehem, Pennsylvania, 1979.

17. Kline, S.J., W.C. Reynolds, F.A. Schraub and P.W. Runstadler. The Structure of Turbulent Boundary Layers. J. Fluid Mech., 30, 1967, pp. 741-773.

18. Kim, H.T., S.J. Kline and W.C. Reynolds. The Production of Turbulence Near a Smooth Wall in a Turbulent Boundary Layer. J. Fluid Mech., 50, 1971, pp. 133-160.

19. Virk, P.S. Drag Reduction Fundamentals. AIChE Journal, 21, 1975, pp. 625-656.

20. Lumley, J.L. Drag Reduction in Two Phase and Polymer Flows. The Physics of Fluids, 20, No. 10, Pt. II, 1977, pp. S64-S71.

21. Fruman, D.H. and M.P. Tulin. Diffusion of a Tangential Drag-Reducing Polymer Injection on a Flat Plate at High Reynolds Numbers. J. of Ship Research, 20, 1976, pp. 171-180.

22. Latto, Brian and Chi-Hung Shen. Experimental Investigation of Polymer Solution Injection on External Boundary Layers. Proceedings of the Symposium on Turbulence Measurements in Liquids, September 1969 ed. by G.K. Patterson and J.L. Zakin, Dept. of Chemical Engrg., University of Missouri-Rolla, 1971, pp. 110-115.

23. Tullis, J.P. and K.L.V. Ramu. Drag Reduction in Developing Pipe Flow with Polymer Injection. BHRA International Conference on Drag Reduction, Sept., 1974, Paper G3.

24. Latto, Brian and O.K.F. ElReidy. Diffusion of Polymer Additives in a Developing Turbulent Boundary Layer. J. Hydronautics, 10, 1976, pp. 135-139.

25. Wu, J., D.H. Fruman and M.P. Tulin. Drag Reduction by Polymer Diffusion at High Reynolds Numbers. J. Hydronautics, 12, 1978, pp. 134-136.

26. Fruman, D.H. and P. Galivel, Near-Field Viscoelastic Effects during Thin-Slit Drag-Reducing Polymer Injection. Journal of Rheology, 24, 1980, pp. 627-646.

27. Fruman, D.H. and P. Galivel. Anomalous Effects Associated with Drag-Reducing Polymer Ejection into Pure-Water Turbulent Boundary Layers. Viscous Flow Drag Reduction, Vol. 72, Progress in Astronautics and Aeronautics, ed. by G.R. Hough. American Institute of Aeronautics and Astronautics, New York, NY, 1980, pp. 332-350.

28. Vleggaar, J. and M. Tels. Drag Reduction by Polymer Threads. Chemical Engineering Sci., 28, 1973, pp. 965-968.

29. Stenberg, L.-G., T. Lagerstedt, O. Sehlen and E.R. Lindgren. Mechanical Mixing of Polymer Additive in Turbulent Drag Reduction. The Physics of Fluids, 20, 1977, pp. 858-859.

30. Stenberg, L.-G., T. Lagerstedt and E.R. Lindgren. Polymer Additive Mixing and Turbulent Drag Reduction. The Physics of Fluids, 20, No. 10, Pt. II, 1977, pp. S276-S279.

31. Offen, G.R. and S.J. Kline. Combined Dye-Streak and Hydrogen-Bubble Visual Observations of a Turbulent Boundary Layer. J. Fluid Mech., 62, 1974, pp. 223-240.

32. Praturi,A.K. and R.S. Brodkey. A Stereoscopic Visual Study of Coherent Structures in Turbulent Shear Flow. J. Fluid Mech., 89, 1978, pp. 251-272.

33. Smith, C.R. Visualization of Turbulent Boundary-Layer Structure Using a Moving Hydrogen Bubble-Wire Probe. Proceedings of the Workshop on Coherent Structure of Turbulent Boundary Layers, Lehigh University, Bethlehem, Pennsylvania, November 1978, pp. 48-94.

34. Nychas, S.G., H.C. Hershey and R.S. Brodkey. A Visual Study of Turbulent Shear Flow. J. Fluid Mech., 61, 1973, pp. 513-540.

35. Falco, R.E. Coherent Motions in the Outer Region of Turbulent Boundary Layers. Physics of Fluids, 20, No. 10, Part II, 1977, S124-S132.

36. Oldaker, D.K. An Experimental Investigation of the Near-Wall Flow Structure During Drag Reduction. M.S. thesis, Oklahoma State University, Stillwater, Oklahoma, December, 1974.

37. Bogard, D.G. and W.G. Tiederman. Investigation of Flow Visualization Techniques for Detecting Turbulent Bursts. Paper presented at the Seventh biennial symposium on turbulence, University of Missouri-Rolla, September, 1981.

APPENDIX A

PROCEDURE FOR CLEANING AND INSTALLING MANOMETERS

1) Drain manometers.
2) Remove all accessories from glassware.
3) Do not force the rubber O-ring if it is swollen.
4) Rinse with deionized and filtered water.
5) Rinse with alcohol - manometer should look very clean to the naked eye at this point.
6) Rinse with deionized and filtered water.
7) Add chromic acid and swirl around. If acid changes color dump and repeat.
8) When acid doesn't change color continue to add acid until manometer is 3/4 full, swirl around for several minutes. For best results, let stand overnight set at angle such that the acid fills both chambers.*
9) Rinse several times with deionized, filtered water-manometer should look very clean.
10) Rinse with alcohol.
11) Rinse syringe with alcohol and dry.
12) Connect syringe to manometer with tygon tubing and draw air in and out until manometer is dry.
13) Install manometer on channel bracket.
14) Using a clean, dry syringe inject 19 to 20 cc of manometer fluid into the right side of the manometer. A long needle should be used so that the fluid does not splash excessively.
15) Carefully add deionized water to the right (lower) side. When the interface has formed continue adding 2 to 3 ml of water.
16) Using another clean syringe and needle suck off the manometer fluid that will be on the air-water interface.
17) Using the first syringe, add water to right side until side outlet is filled-attach hose to that outlet and clamp off.
18) Repeat steps 15), 16), and 17) for left side. The micrometer will have to be attached to the right tube as water reaches the top of that outlet.

Note: The manometer will remain clean for 4 to 6 days if hoses are not hooked up to the channel. Once hooked up to the channel the dissolved salts in the channel water will "dirty up" the manometer interface and walls.

*Much better cleaning obtained by placing manometers filled with chromic acid into water (outlets not submerged) and boiling the water.

APPENDIX B

PREPARATION OF 100 PPM POLYMER SOLUTIONS

This procedure prepares 32 liters of solution.

1) Heat 4 liter of filtered tap water to boiling.
2) Allow water to cool to 90-100°F.
3) Mix 3.20 grams of SEPARAN AP-273 with about 25 ml of isopropyl alcohol in a separate beaker.
4) With a magnetic stirrer, stir water at a high rate but be careful not to entrain any air.
5) Swirl the alcohol-polymer mixture until the polymer is suspended in the alcohol. In one motion pour the entire contents into the swirling water slightly off center of the vortex.
6) Continue to stir at a reduced rate until all large clumps of the polymer are dispersed. This requires 5 to 15 minutes.
7) Allow the solution to hydrate for 12 to 24 hours. The solution should be completely clear at the end of this period.
8) Dilute the concentrated solution with 28 liters of filtered tap water and allow the diluted solution to hydrate for 12 to 24 hours before using.

To prepare 32 liters of 400 ppm solution, use 12.8 grams of AP-273, 100 ml of isopropyl alcohol, 5 liters of boiled water and 27 liters of water for dilution.

SYMBOLS

b - Spanwise distance over which streaks were counted

c_f - Skin friction coefficient, defined by Equation (7).

D - Internal diameter of tube.

DR - Per cent drag reduction, defined by Equation (10).

g - Acceleration of gravity

h - Manometer deflection without injection.

h_i - Manometer deflection during injection.

ℓ - Estimated average length of a streak.

$\overline{N}$ - Average number of streaks.

P - Static pressure.

Re - Reynolds number.

U - Bulk or mass average velocity.

v^* - Shear velocity, defined by Equation (2).

x - Streamwise co-ordinate with the origin at the slots.

y - Co-ordinate normal to the wall

Greek

Δ - Difference in the quantity that follows the symbol.

λ - Spanwise spacing.

μ - Viscosity

ν - Kinematic viscosity

ρ - Density

τ_w - Wall shear stress

Superscript

$+$ - Indicates that the quantity has been made dimensionless by using the shear velocity and kinematic viscosity.